ISSN: 2472-3703 DOI: 10.6911/WSRJ.202308_9(8).0004

Design and Simulation of Double Closed Loop DC Speed Control System for Digital Control PWM-M System

Yuping Jiang[1, a]

[1]Electrical Engineering and Automation, North China University of Technology, Beijing, 100144, China

[a]fzjypfzjyp@163.com

Abstract

Using engineering design method, the speed and current double closed-loop DC speed regulation system is designed, and simulink is used to simulate the system. Finally, through the analysis of the simulation results, the four-quadrant running diagram of torque speed is also observed, and its working principle is analyzed. The simulation overshoot and waveform are roughly the same as the theory, and the double closed loop has better rapidity, stability and accuracy, which further verifies the superiority of the double closed loop speed regulation system.

Keywords

Double closed loop, Simulink, PI control, DC speed regulation system.

1. INTRODUCTION

Dc motor because of its performance is suitable for a wide range of smooth speed control, its speed control system has always played an extremely important role in industrial control. The most typical DC speed control system is the speed and current double closed-loop speed control system[1]. The double closed loop speed control system is the mainstream equipment in the DC motor speed control system. It has the advantages of wide speed control range, good stability and high precision. It is a mature system in both theory and practice. Since the 1970s, it has been increasingly widely used in metallurgy, machinery, manufacturing and printing and dyeing industry in China[2]. In this paper, the double closed-loop speed control system is designed by using engineering design method, and simulink tool in matlab is used to simulate the system and test its performance.

2. DESIGN REQUIREMENTS

The Simulink simulation model of digital control PWM-M system with double closed-loop DC speed regulation is designed in this paper[3],Controllable DC power supply adopts reversible PWM converter.Peak phase voltage of the three-phase AC power U_{peak}is160V.Dc power supply is obtained by using three-phase diode uncontrolled rectificationU_s， The DC bus capacitance is 1F.In PWM generator, the triangular carrier frequency is 5kHz.Current feedback filtering time constant T_{0i}=0.0006s,Speed feedback filtering time constant T_{0n}=0.002s.Regulator maximum allowable current of ASR's saturated output motor $I_{dm}=\lambda I_N=1.5I_N$。 ACR saturation output motor maximum armature voltage $U_{dm}=U_s$.Dc motor parameter selection preset model 6,It can be seen from the table that the model parameters are as follows (as the table 1).C_e=0.12.The dynamic index of the system is: current overshoot $\sigma_i \le 7\%$,Speed over regulation from full load start to rated speed $\sigma_n \le 5\%$.

World Scientific Research Journal Volume 9 Issue 8, 2023
ISSN: 2472-3703 DOI: 10.6911/WSRJ.202308_9(8).0004

Table 1. Model 6 Motor parameters

Preset model	P_N (kW)	n_N (r/min)	U_N (V)	I_N (A)	T_N (N.m)	R_a (Ω)	L_a (mH)	J (Kg. m^2)
06	14.914	1750	240	73	81.39	0.4114	4.895	0.08321

3. SPECIFIC DESIGN

3.1. Automatic current regulator design

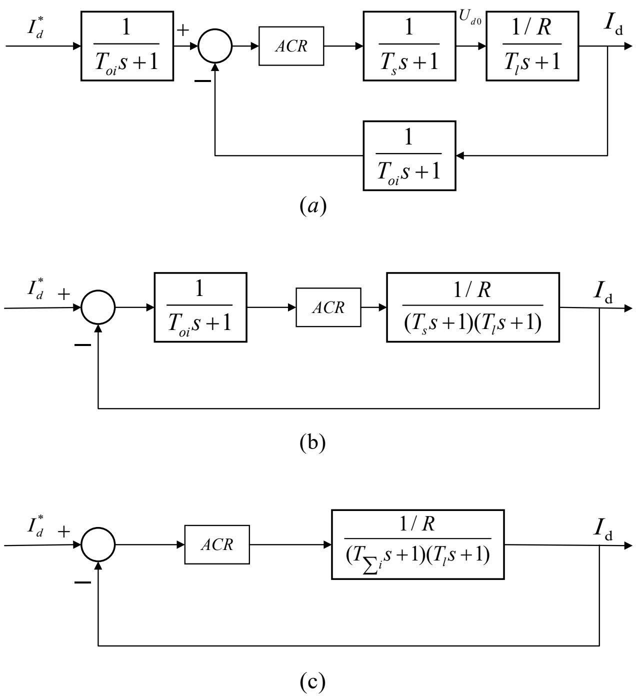

Figure 1. Dynamic structure diagram of Automatic current regulator and its simplification

The dynamic structure of the Current loop is shown in the figure 1. From the perspective of steady-state performance, it is hoped that the Current loop can achieve no static current difference to obtain ideal locked rotor characteristics; From the dynamic point of view, more attention is paid to the following performance of the Current loop, that is, the smaller the current overshoot, the better. In comprehensive consideration, the Current loop should be corrected to a typical type I system[4],The calculation steps for selecting the PI regulator for ACR are as follows.The open loop transfer function of the Current loop is

$$G_{0i}(s)=\frac{k_i(\tau_i s+1)}{\tau_i s}\frac{\frac{1}{R}}{(T_{\Sigma i}s+1)(T_L s+1)}=\frac{K}{s(Ts+1)}$$

$\tau_i=T_L=0.0119s$, eliminate large inertia links， then there are $T=T_{\Sigma i}=0.0008s$, $K=\frac{k_i}{\tau_i R}$;

Because $KT=0.5$, then there is $K=\frac{0.5}{T}=\frac{0.5}{0.0008}=625$

Then $k_i=K\tau_i R=625\times0.0119\times0.4114=3.06$

So there is $\frac{k_i}{\tau_i}=\frac{3.06}{0.0119}\approx257.14$

Overall $\tau_i=0.0119s$， $k_i=3.06$， $\frac{k_i}{\tau_i}\approx257.14$ ($\sigma=0\%$)

Carry out approximate processing verification, because the cut-off frequency of Current loop is $\omega_{ci}=K=625(s^{-1})$

1.Approximate processing conditions for verifying rectifiers:

$$\omega_{ci}=625(s^{-1})\leq\frac{1}{3T_s}=\frac{1}{3\times0.0002}\approx1666.67(s^{-1})$$

Satisfy approximate conditions.

2.Check the condition of ignoring the dynamic influence of Counter-electromotive force change on Current loop:

$$\omega_{ci}=625(s^{-1})\geq3\sqrt{\frac{1}{T_mT_L}}=3\times\sqrt{\frac{1}{0.026\times0.0119}}\approx170.6(s^{-1})$$

Satisfy approximate conditions.

3.Approximate processing conditions for verifying small time constant of Current loop:

$$\omega_{ci}=625(s^{-1})\leq\frac{1}{3}\sqrt{\frac{1}{T_sT_{oi}}}=\frac{1}{3}\times\sqrt{\frac{1}{0.0002\times0.0006}}\approx962.25(s^{-1})$$

Satisfy approximate conditions.

In summary, parameter calculation dinner, current inner ring design completed.

3.2. Automatic speed regulator Design

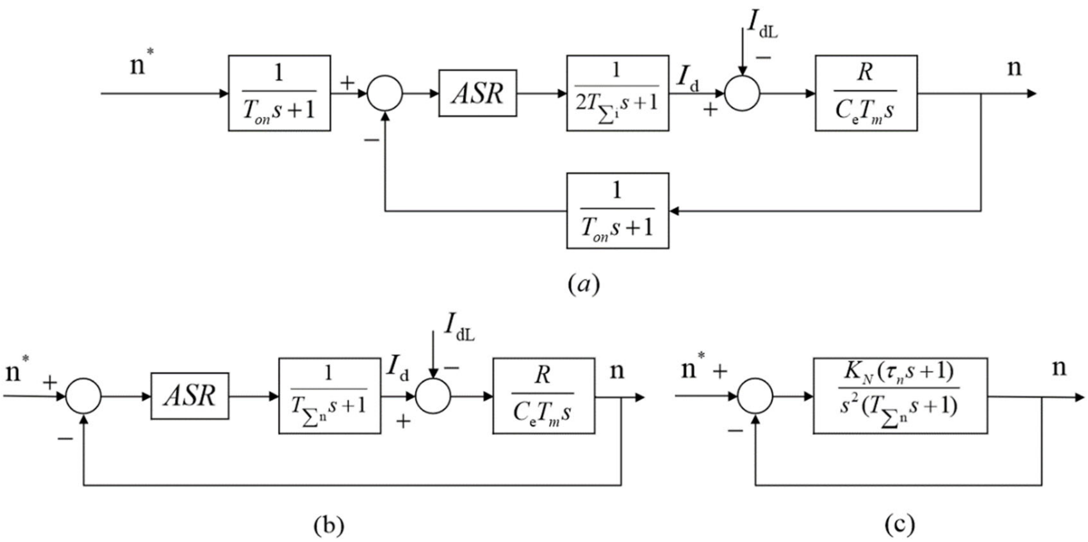

Figure 2. Dynamic Structure Diagram and Simplification of Automatic speed regulator

(1) Reduced Order Approximation of Current Closed Loop Transfer Function

The dynamic structure diagram of the speed ring is shown in the figure above, from which the current closed-loop transfer function can be obtained as

$$W_{ci}(s)=\frac{1}{2T_{\sum i}^2s^2+2T_{\sum i}s+1}\approx\frac{1}{2T_{\sum i}s+1}$$

The approximate processing conditions is

$$\omega_{cn}\leq\frac{1}{3\sqrt{2}T_{\sum i}}$$

ISSN: 2472-3703 DOI: 10.6911/WSRJ.202308_9(8).0004

(2) Approximate processing of small time constants in the speed loop

$$T_{\sum n}=T_{on}+2T_{\sum i}=0.002+0.0016=0.0036s$$

(3) Parameter tuning of automatic speed regulator

From the perspective of steady-state performance, in order to achieve no static speed difference, there must be an integration link before the interference point of the speed control loop; From the perspective of dynamic performance, more emphasis is placed on the anti-interference performance of the speed loop; The anti-interference performance of the typical II system is superior to that of the typical I system. Comprehensive consideration, the Current loop is designed according to the I type system[5], ASR selects a PI regulator, and the calculation steps are as follows. The open-loop transfer function of the speed loop is

$$G_{on}(s)=\frac{k_n(\tau_n s+1)}{\tau_n s}\frac{1}{T_{\sum n}s+1}\frac{R}{C_e T_m s}=\frac{K(\tau s+1)}{s^2(Ts+1)},$$

$$\tau=\tau_n,\quad T=T_{\sum n},\quad K=\frac{k_n R}{C_e T_m \tau_n};$$

According to the principle that the typical Type II system has good following performance and anti-interference performance, the intermediate frequency width h=5 is taken.

So the time constant is $\tau_n=hT_{\sum n}=5\times0.0036=0.018s$

Open Loop Gain

$$k=\frac{h+1}{2h^2T^2}=\frac{6}{2\times25\times0.0036^2}\approx 9259.26$$

Proportional coefficient of speed regulator

$$k_n=\frac{KC_e T_m \tau_n}{R}=\frac{9259.26\times0.12\times0.026\times0.018}{0.4114}\approx1.264$$

Overall $k_n\approx1.264$ $\tau_n=0.018s$,so there is

$$\frac{k_n}{\tau_n}=\frac{1.264}{0.018}\approx70.2$$

(4) Approximate processing verification

The cut-off frequency of the speed ring is

$$\omega_{cn}=\frac{K}{\omega_1}=K\tau_n=9259.26\times0.02=185.1852(s^{-1})$$

1.Check the approximate processing conditions of Current loop

$$\omega_{cn}\leq\frac{1}{3\sqrt{2}T_{\sum i}}=\frac{1}{3\times\sqrt{2}\times0.0008}=294.6(s^{-1})$$

Satisfy approximate conditions.

2.Approximate processing conditions for verifying small time constants

$$\omega_{cn}\leq\frac{1}{3}\sqrt{\frac{1}{2T_{\sum i}T_{on}}}=\frac{1}{3}\sqrt{\frac{1}{2\times0.0008\times0.002}}\approx186.3(s^{-1})$$

Satisfy approximate conditions.

To sum up, the design of Current loop and speed loop has been completed, and then the model is built and simulated.

World Scientific Research Journal Volume 9 Issue 8, 2023
ISSN: 2472-3703 DOI: 10.6911/WSRJ.202308_9(8).0004

4. MODEL SIMULATION UNDER SIMULINK

4.1. Model construction

Based on the above design, the simulation model built is as Figure 3.

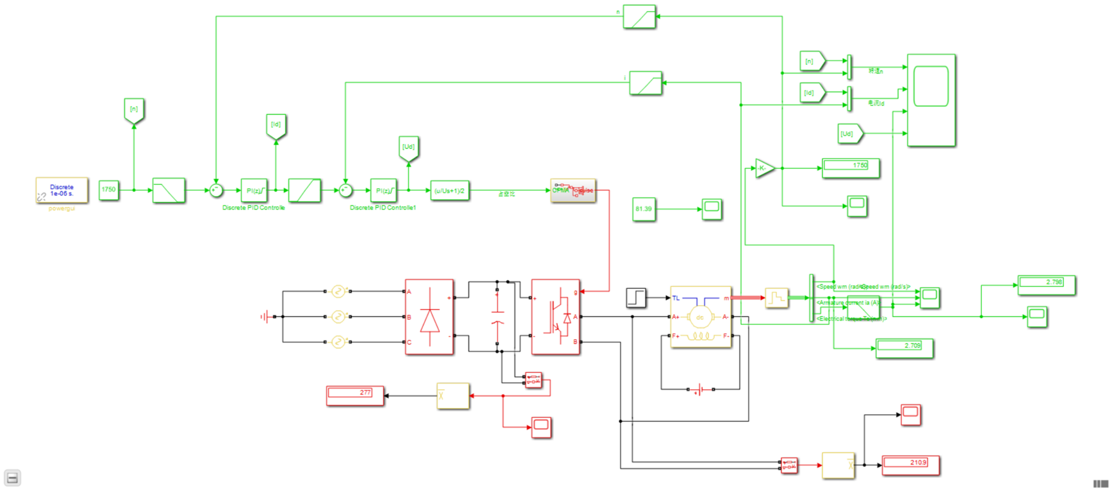

Figure 3. Simulink simulation model for dual closed-loop DC speed regulation of digital controlled PWM-M system

4.2. Experimental analysis of the model

(1) Build a system simulation model on the Matlab/Simulink simulation platform. 0.5 second rated speed step setting gives the simulation waveform (including speed setting waveform, speed feedback waveform, current setting waveform and current feedback waveform) when the speed regulator has anti Integral windup and no anti Integral windup during no-load starting to rated speed. The experimental waveform is as follows.

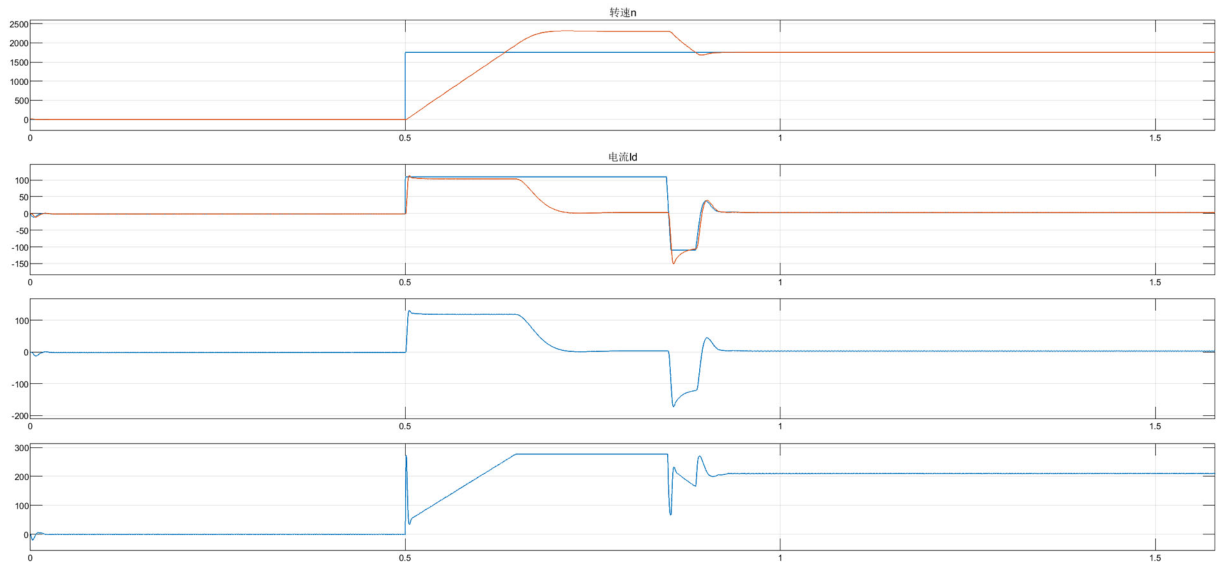

Figure 4. Simulation waveform of speed regulator without anti Integral windup

ISSN: 2472-3703 DOI: 10.6911/WSRJ.202308_9(8).0004

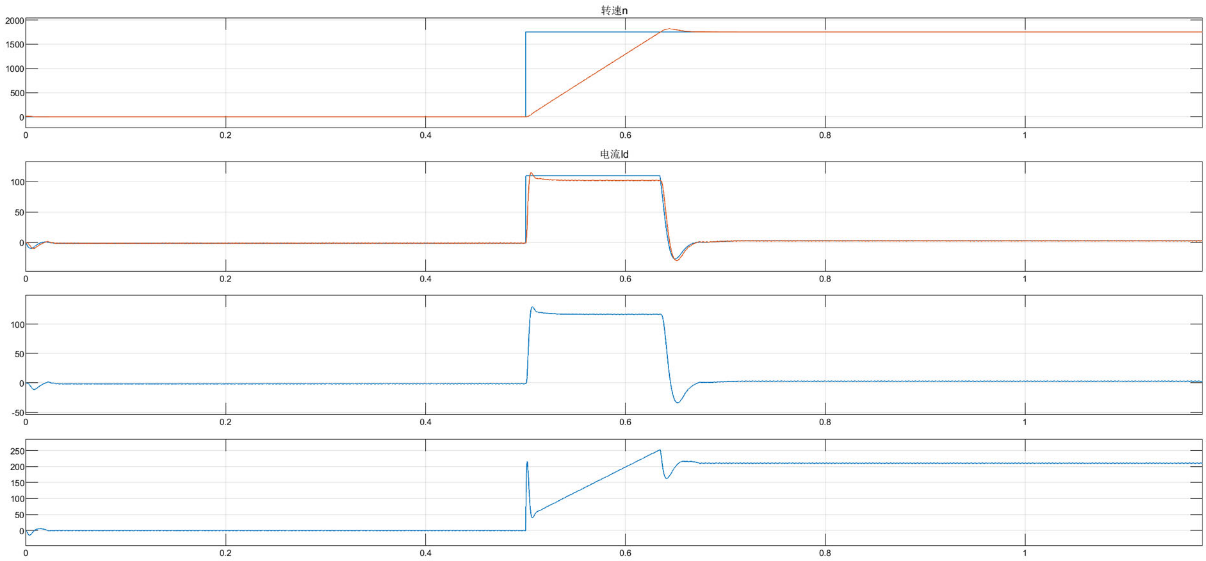

Figure 5. Speed regulator has simulation waveform against Integral windup

According to Figures 4 and 5, the speed overshoot of the simulation waveform with anti Integral windup is significantly smaller than that of the simulation waveform without anti Integral windup. The specific reason is that PI regulators with anti Integral windup have set integral limits, which can limit the accumulation of integrals all the time. PI regulators without anti Integral windup may have large integral terms due to accumulation, so they will eventually have large desaturation overshoot.

(2) If the current inner loop is designed according to the Type I system, in order to ensure that the current overshoot is $\sigma_i \leq 7\%$,let KT=0.5， At this point, the theoretical overshoot should be around 4.3%.Given a 0.5 second rated speed step, the current setting and current feedback simulation waveform during no-load starting are given as follows, and the current overshoot is measured.

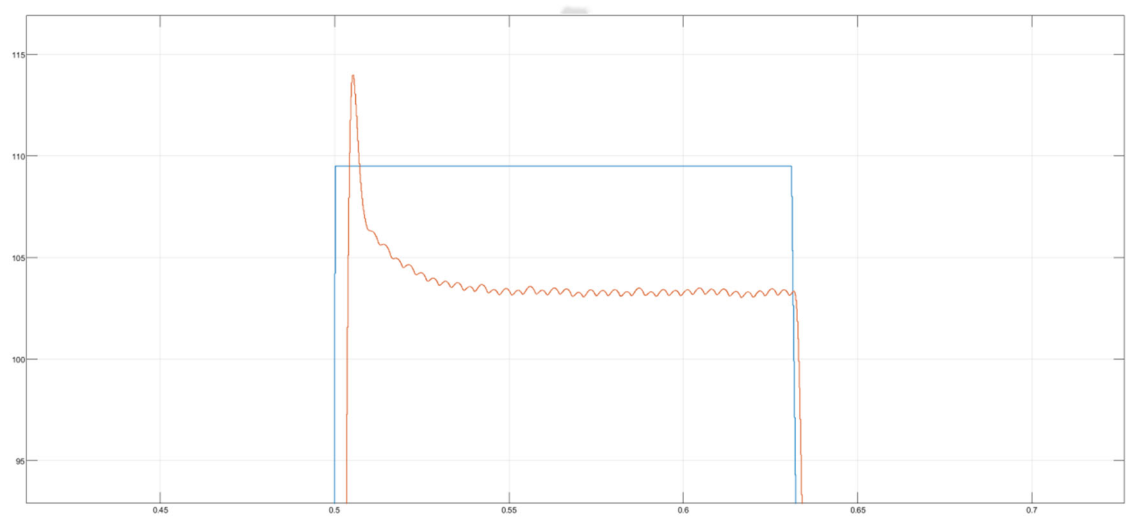

Figure 6. Simulation Waveform of No-load Starting Current Setting and Current Feedback

ISSN: 2472-3703 DOI: 10.6911/WSRJ.202308_9(8).0004

The current overshoot can be calculated as the Figure 6.

$$\sigma_i = \frac{i_1 - i_2}{i_2} = \frac{114-109.5}{109.5} \approx 4.1\%$$

So the simulation results are roughly the same as the theoretical calculation of 4.3%, and the overshoot of the simulation model is required to meet the theoretical calculation.

(3) Given a 0.5 second rated speed step, the motor starts with no load to the rated speed, and suddenly applies a gravity rated load at 1.5 seconds.Through simulation, it can be concluded that the simulated dynamic speed drop is

$$\Delta n = 1750 - 1693 \approx 57 \text{ r/min}$$

The calculation process of the theoretical speed dynamic speed dropΔn is as follows:

$$\Delta n_b = 2FK_2 T = 2\frac{T_N}{9.55C_e}\frac{R}{C_e T_m}T_{\Sigma n}$$

$$= 2 \times \frac{81.39}{9.55 \times 0.12} \times \frac{0.4114}{0.12 \times 0.026} \times 0.0036 = 67.41 \text{r/min}$$

$$\Delta n = \frac{\Delta C_{max}}{C_b}\Delta n_b = 0.812 \times 67.41 \approx 54.7 \text{ r/min}$$

It can be seen that the error between the simulation results and the theoretical values is small, and there is no problem with building the model.

(4) The rated speed step is given, and after the motor starts with gravity rated load and stabilizes at the rated speed, the speed given n^*drops from 1750 rpm to -1750 rpm,Store the data of electromagnetic torque T_e, motor speed n, and load torque T_L during the stable operation of the motor from start to reverse through an oscilloscope in the workspace, and draw and capture the speed torque quadrant diagram as follows.

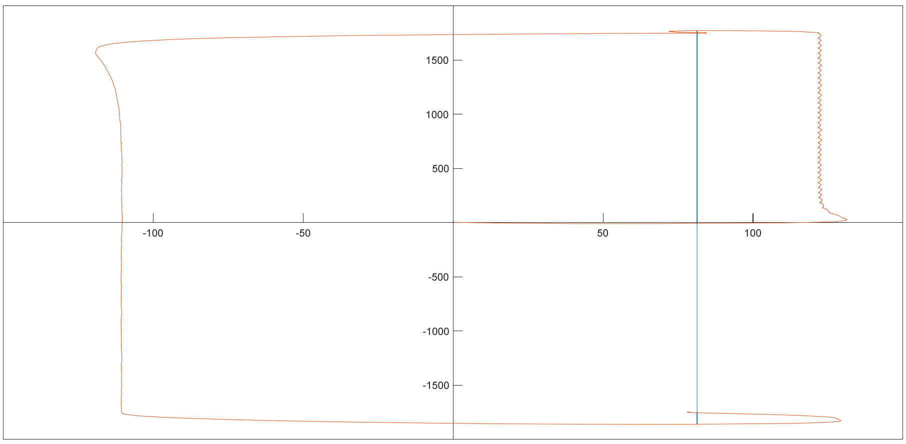

Figure 7. Speed torque four quadrant operation diagram

Through experiments, the rated speed step is given, and after the motor is started with gravity rated load and stable operation at rated speed, the speed given n^* drops from 1750 rpm to -1750 rpm, as shown in the speed torque quadrant diagram in Figure 7.

ISSN: 2472-3703 DOI: 10.6911/WSRJ.202308_9(8).0004

Below is an analysis of the entire process: during startup, it can be seen that the electromagnetic torque is very high, causing a linear increase in speed. At this time, the electromagnetic torque is the driving torque, and the load torque is the braking torque. The motor operates in a forward electric state and operates in the first quadrant. This speed regulator quickly enters a saturation state, at which point the motor starts at the maximum allowable starting current, and the motor speed also increases rapidly. After the motor speed reaches the given speed, the armature current decreases, but at this time, the motor is still accelerating, so the speed will be greater than the rated speed, causing a desaturation overshoot, and ultimately the motor will stabilize at 1750r/min.

When the speed drops suddenly from 1750 rpm to -1750 rpm, the forward armature current decays first. At this time, the motor speed slowly decreases to 0, and both the electromagnetic torque and load torque are braking torques. The motor operates in the forward braking state and operates in the second quadrant. Afterwards, when the speed changes from 0 to negative, the system starts the motor in reverse with a negative constant current. At this time, the electromagnetic torque and load torque are both driving torques, and the motor operates in a reverse electric state, operating in the third quadrant. Accelerate in reverse until the given speed is reached. At this time, the electromagnetic torque is the braking torque, and the load torque is the driving torque. The motor operates in a reverse braking state and operates in the fourth quadrant. The load torque and electromagnetic torque are equal in magnitude and opposite in direction, and the motor operates stably in reverse.

5. CONCLUSION

This article adopts the engineering design method to design a dual closed-loop DC speed control system; And combined with the Simulink tool, the system was simulated; Through the speed simulation image, it can be visually seen that the system can achieve reversible operation and has good speed, stability, and accuracy; Moreover, the overshoot meets the design requirements, which further verifies the superiority of the dual closed-loop speed control system.

REFERENCES

[1] Boshi Chen:Electric traction automatic control system: motion control system Mechanical Industry Press, 2003.9-10.

[2] Shaoyong Cao Design and Simulation of a Double Closed Loop Speed Control System for Brushless DC Motors. Explosion proof Motors 43.3(2008):5.6.

[3] Shengqian Liu et al "Modeling and simulation of double closed loop DC speed regulating system based on MATLAB." Journal of Guilin University of Technology 36.2(2016):5.63.

[4] Zhenyan Zhang, and Rui Zuo Design and Simulation of Double Closed Loop DC Speed Control System. Development and Innovation of Mechanical and Electrical Products 5(2011):3.98-99.

[5] Jian Jiao. “Simulation Design of Double Closed Loop PWM Reversible DC Speed Control System”. Electronic Technology (Shanghai) 51.8(2022):3.58-60.